CHEMICAL ENGINEERING TRANSACTIONS
VOL. 43, 2015
A publication of AIDIC
The Italian Association of Chemical Engineering
Online at www.aidic.it/cet
Chief Editors: Sauro Pierucci, Jiří J. Klemeš

**ISBN** 978-88-95608-34-1; **ISSN** 2283-9216
DOI: 10.3303/CET1543123

# Electrochemical $H_2O_2$ Sensors Based on Au/$CeO_2$ Nanoparticles for Industrial Applications

Claudio Ampelli*[a], Salvatore G. Leonardi[b], Anna Bonavita[b], Chiara Genovese[a], Georgia Papanikolaou[a], Siglinda Perathoner[a], Gabriele Centi[a], Giovanni Neri[b]

[a]Dep. of Electronic Engineering, Industrial Chemistry and Engineering, University of Messina, v.le F. Stagno d'Alcontres, 31 - 98166 Messina, Italy
[b]Dep. of Electronic Engineering, Industrial Chemistry and Engineering, University of Messina, c.da di Dio - 98166 Messina, Italy
ampellic@unime.it

Gold-cerium oxide (Au/$CeO_2$) composite was synthesized by a deposition-precipitation method and used to fabricate a highly sensitive non-enzymatic electrochemical sensor for hydrogen peroxide ($H_2O_2$) detection. The morphology and microstructure of the Au/$CeO_2$ composite was characterized by transmission electron microscopy (TEM) and X-ray diffraction (XRD). UV-Vis spectroscopy showed a strong plasmonic absorbance (in the range of 500-650 nm) due to Au nanoparticles deposited onto the surface of ceria. Sensing tests carried out by cyclic voltammetry (CV) showed that the Au/$CeO_2$-composite-modified screen-printed carbon electrode exhibited electrocatalytic response to $H_2O_2$. By chronoamperometry, a detection limit (S/N=3) as low as 5 μM and a sensitivity of 27.1 μA $mM^{-1}cm^{-2}$ were measured. These results open the route for a potential use of the fabricated Au/$CeO_2$-based sensor to improve the $H_2O_2$ detection ability in many industrial fields.

## 1. Introduction

The analytical determination of hydrogen peroxide ($H_2O_2$) is of great importance in environmental, pharmaceutical and industrial fields (Kim et al., 2013). From municipal wastewater and drinking water treatments to gas, oil and petrochemical refinery applications, polymer product manufacture, wood pulp, paper and milling industries as a bleaching agent, $H_2O_2$ is playing a major role in the modern industrial world (Jones, 1999).
Electrochemical sensors for $H_2O_2$ detection are basically classified into two major categories: enzymatic and non-enzymatic sensors. Although enzyme-based electrochemical biosensors are still dominating, they are affected by temperature, pH and toxic chemicals (Ensafi et al., 2015). On the other hand, in recent years, nanomaterials have attracted great research interest because of their desirable chemical, physical and electronic properties that are different from those of bulk materials (Ampelli et al., 2014a). They have also attracted a remarkable interest for their simplicity and low cost (Ampelli et al., 2014b). The electrocatalytic properties of enzyme-free electrochemical sensors can be improved by using suitable nanomaterials to modify the working electrode, enhancing the current and decreasing the high over-potentials of many compounds which downgrade the sensing performance in common unmodified electrodes (Chen et al., 2013).
A large range of nanomaterials such as metals, metal oxides, carbon nanotubes, graphene, and also nanocomposite materials, have been employed for electrocatalytic $H_2O_2$ detection (Leonardi et al., 2014). For example, Yi et al. (2011) fabricated $H_2O_2$ sensors based on highly ordered Ag-nanoparticle-decorated silicon nanowire arrays, obtaining favourable electrocatalytic performance due to their high electrical conductibility. Zhao et al. (2009) fabricated $H_2O_2$ sensors based on multiwalled carbon nanotubes/Ag nanohybrids modified gold electrode, obtaining high sensitivity and reducing interferences from other oxidizable species. Among the metal oxides, ceria ($CeO_2$) is one of the most promising semiconductor oxide material for biosensor fabrication due to its excellent properties, including good biocompatibility, high chemical stability and excellent electronic

Please cite this article as: Ampelli C., Leonardi S., Bonavita A., Genovese C., Papanikolaou G., Perathoner S., Centi G., Neri G., 2015, Electrochemical h2o2 sensors based on au/ceo2 nanoparticles for industrial applications, Chemical Engineering Transactions, 43, 733-738
DOI: 10.3303/CET1543123

conductivity (Zhang et al., 2012). Ispas et al. (2008) prepared uniform colloidal ceria nanoparticles and described new possibilities of exploring the unique catalytic and redox properties of this material for the development of a simple enzymeless sensor for the determination of $H_2O_2$. Ujjain et al. (2014) prepared ceria nanoparticles by hydrothermal treatments using different capping agents. They found that $CeO_2$-HMTA, synthesized by the use of hexamethylene-tetra-amine (HMTA), exhibited superior electrocatalytic activity toward $H_2O_2$ reduction, due to its better microstructural characteristics. Furthermore, by amperometric responses they measured a sensitivity of 27.1 μA $cm^{-2}$ $mM^{-1}$.
The presence of noble metal nanoparticles (NPs) may significantly improve the sensing performance (Ampelli et al., 2012). Au/$CeO_2$ has shown a remarkable electrocatalytic activity towards some biomolecules such as dopamine (Tong et al., 2013). Au/$CeO_2$/chitosan was used as enzymatic $H_2O_2$ sensor (Zhang et al., 2012) but, to the best of our knowledge, no noble-metal-doped $CeO_2$ material was yet used as electrode for $H_2O_2$ electrooxidation detection.
In this contribution we report on the fabrication of $H_2O_2$ sensors based on Au NPs dispersed on $CeO_2$ by a deposition-precipitation method. The electrochemical sensors were manufactured by printing Au/$CeO_2$ composites onto commercial carbon-based planar electrodes and tested by cyclic voltammetry in the presence of $H_2O_2$ to evaluate their electrochemical performances. The main aim is to fabricate an electrochemical sensor showing favourable electrocatalytic performances in terms of high sensitivity, facile preparation procedure, wide linear range, low limit of detection, long-term stability, satisfying reproducibility and anti-interference ability, providing a promising platform for non-enzymatic sensing of $H_2O_2$.

## 2. Experimental

### 2.1 Preparation and characterization of Au/$CeO_2$ nanocomposite

The electrode materials were prepared by depositing Au NPs onto commercial $CeO_2$ (powder, supplied by STREM Chemicals) by a deposition-precipitation method (Signoretto et al., 2013). In particular, the oxide support was suspended in an aqueous solution of the Au precursor ($HAuCl_4 \cdot 3H_2O$) for 3 h at pH 8.6. The pH was controlled and adjusted by adding NaOH (0.5 M). The sample was washed, filtered and dried at 35 °C for 12 h and finally reduced at 200 °C. The final Au loading onto $CeO_2$ was 1.5 wt. %.
The sensing materials were characterized by X-Ray Diffraction (XRD) using a D2 Phaser Bruker diffractometer equipped with a Cu-Kα radiation source and operated at 30 kV and 10 mA. Data were collected at a scanning rate of 0.025° $s^{-1}$ in a 2θ range from 12° to 100°. Transmission Electron Microscopy (TEM) images were acquired by the use of a Joel JEM 2010 electron microscope with an accelerating voltage of 200 keV. Ultraviolet-visible diffuse reflectance spectra were recorded by a Jasco V570 spectrometer equipped with an integrating sphere for solid samples using $BaSO_4$ as reference and in air. The particle size was calculated using the Scherrer equation.

### 2.2 Preparation of Au/$CeO_2$-modified electrode

Water suspensions of the synthesized Au/$CeO_2$ composites were mixed with Nafion (5 wt. %) and sonicated for 15 min in order to obtain a homogeneous dispersion. The suspensions were then printed on the working electrode of a disposable planar sensor (supplied by Dropsens) consisting of three electrodes, namely a carbon screen-printed working electrode (4 mm diameter), a carbon auxiliary electrode and a silver pseudo-reference electrode. The printed sensors were then allowed to dry at room temperature.

### 2.3 $H_2O_2$ sensing tests

The electrochemical measurements were performed by means of a Dropsens μStat 400 potentiostat. The so-fabricated sensors were characterized by cyclic voltammetry (CV) and chrono-amperometric tests in a pH 7.4 phosphate buffer solution (PBS). CV tests were carried out at different scan rates (50-500 mV $s^{-1}$) in the range of potentials between –0.8 V and 0.8 V, in the presence of different concentrations of $H_2O_2$ in PBS (0-25 mM). Chrono-amperometric curves were obtained recording the oxidation current at a fixed potential, while an appropriate volume of $H_2O_2$ solution was added into the PBS maintained under magnetic stirring conditions.

## 3. Results and discussion

### 3.1 Characterization of Au/$CeO_2$ nanocomposite

The morphology and size of the synthesized Au/$CeO_2$ sample was elucidated by the TEM images shown in Figure 1. The TEM images of the composite sample show large aggregates of $CeO_2$ nanoparticles. The aggregates are composed of grains with a prismatic-like shape and an average size of ~10-15 nm.

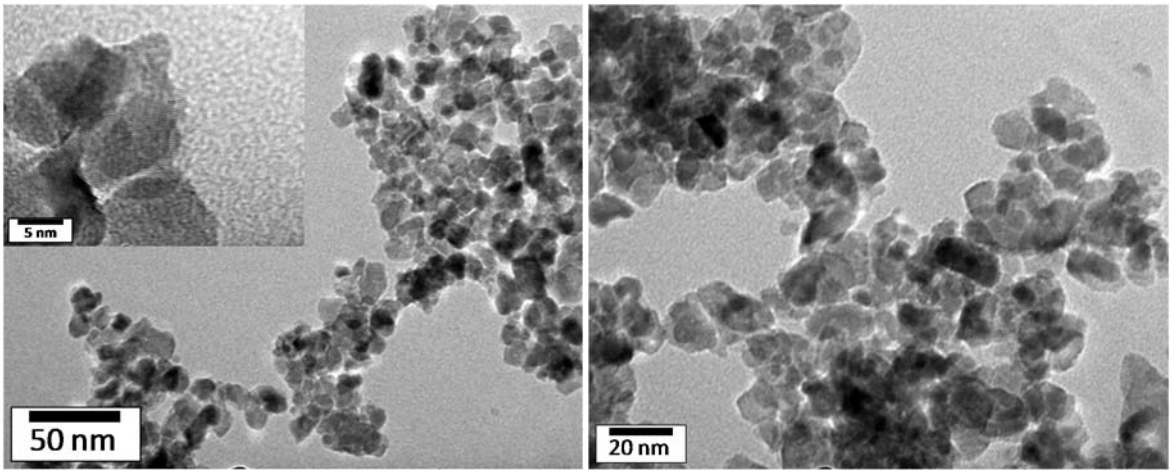


*Figure 1: Representative TEM images of the Au/$CeO_2$ sample. The inset in the figure on the left shows lattice fringes of the $CeO_2$ nanoparticles*

The high-resolution image in the inset shows the lattice fringes of the $CeO_2$ nanoparticles, suggesting their crystalline nature. Small gold NPs are also occasionally visible on the surface of the $CeO_2$ grains.
XRD gives information about the crystal structures and phase of the crystalline material synthesized. The general feature of the XRD patterns, in particular the presence of strong and sharp peaks, confirm that the $CeO_2$ nanoparticles are crystalline (Figure 2a). The XRD spectra display sharp peaks situated at $2\theta$ = 28.6, 33.2, 47.5, 56.5, 59.2, 69.4, 76.7, and 79.1, which are corresponding to (111), (200), (220), (311), (222), (400), (331) and (420) planes, respectively. The values of d-spacing are in good agreement with that of $CeO_2$ in its face-centred cubic phase (JCPDF cards no 75-8371) (Palard et al., 2010). The average diameter of $CeO_2$, as calculated by the use of the Scherrer equation, is about 12.0 nm, which is in according with the TEM results. The XRD pattern of the composite sample also exhibits the characteristic peak of metallic Au at about $2\theta$ = 38.5. The peak of metallic Au shows a weak intensity, due either to the low Au loading (1.5 wt. %) or to low crystallinity.
UV-Vis characterization has also been performed to get further information about the Au NPs supported on $CeO_2$. Figure 2b shows the UV-visible diffuse reflectance spectrum of the Au/$CeO_2$ sample (the spectrum of pure $CeO_2$ is also shown as a comparison). The intense band below 400 nm is due to the typical absorption of the $CeO_2$ semiconductor, while the broad band in the visible region (in the range of 500-650 nm) is attributable to the presence of Au NPs on the surface of ceria. It is well known that Au NPs absorb light in the visible region due to Localized Surface Plasmon Resonance (LSPR) effect. LSPR refers to the collective oscillation of free conduction band electrons of the Au NPs (Ampelli et al., 2014c). It is to remark that this band is not usually observed in gold bulk materials and that Au NPs deposited onto a $CeO_2$ surface show very peculiar properties (Ampelli et al., 2014d).

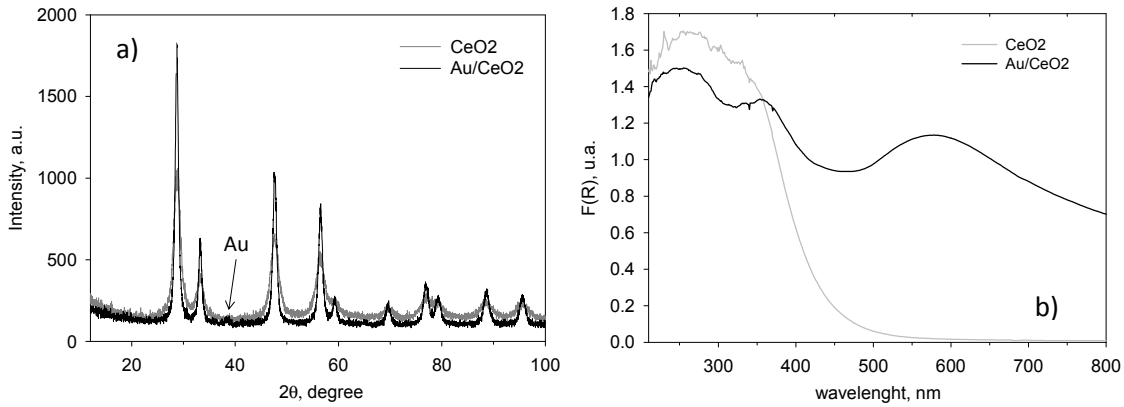


*Figure: 2: a) XRD patterns and b) UV-Visible diffusive reflectance spectra of Au/$CeO_2$ and $CeO_2$ samples*

The strong plasmon resonance effect observed may be attributed to the interfacial interactions between Au and $CeO_2$, resulting in the electron and energy transfer from the metal surface to the semiconductor material (Zhang et al., 2012).

### 3.2 $H_2O_2$ sensing tests

The synthesized Au/$CeO_2$ composite was then used to modify the working electrode of a disposable carbon electrode and tested for the electrooxidation of $H_2O_2$. In order to evaluate the role of Au in the $CeO_2$ matrix, CV experiments were first carried out on the bare carbon electrode and pure-$CeO_2$-modified electrode. It was observed that both the bare carbon electrode (not shown) and pure $CeO_2$ do not contribute to the electrooxidation activity towards this analyte in the operating conditions adopted. No evident current peaks, in fact, were observed at a potential of about 0.6 V (Figure 3a). This agrees with recent results reported by Ispas et al. (2008), who, investigating $CeO_2$ nanoparticles for $H_2O_2$ detection at different pH, noted a higher electrocatalytic activity when working in alkaline medium than when the pH was nearly neutral.
The CV of the Au/$CeO_2$ nanocomposite in the presence of hydrogen peroxide shows instead a clear anodic peak at about 0.6 V (Figure 3a). Figure 3b shows the CV curves recorded at different scan rates from 25 to 400 mV $s^{-1}$, while the inset shows a plot of the peak current (at ~0.6 V) vs. the square root of the scan rate. A linear relationship between the peak current and the square root of the scan rate in this scan-rate range was obtained, indicating that the process of electrooxidation is controlled by diffusion.

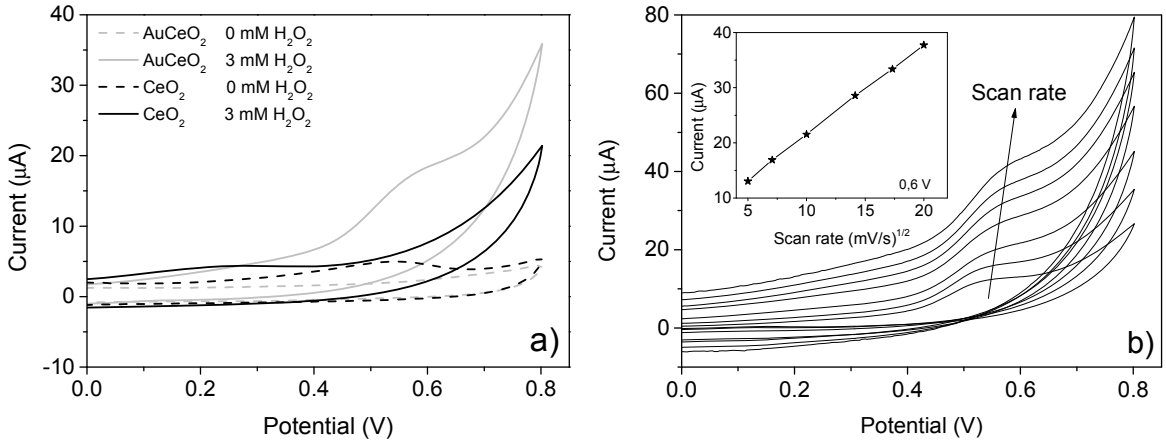


*Figure 3: a) CVs of $CeO_2$ nanoparticles and of Au/$CeO_2$ nanocomposite in the absence and presence of hydrogen peroxide; b) CVs of Au/$CeO_2$ nanocomposite in the presence of 3 mM hydrogen peroxide at different scan rates; inset in b) plot of the peak current vs. the square root of the scan rate*

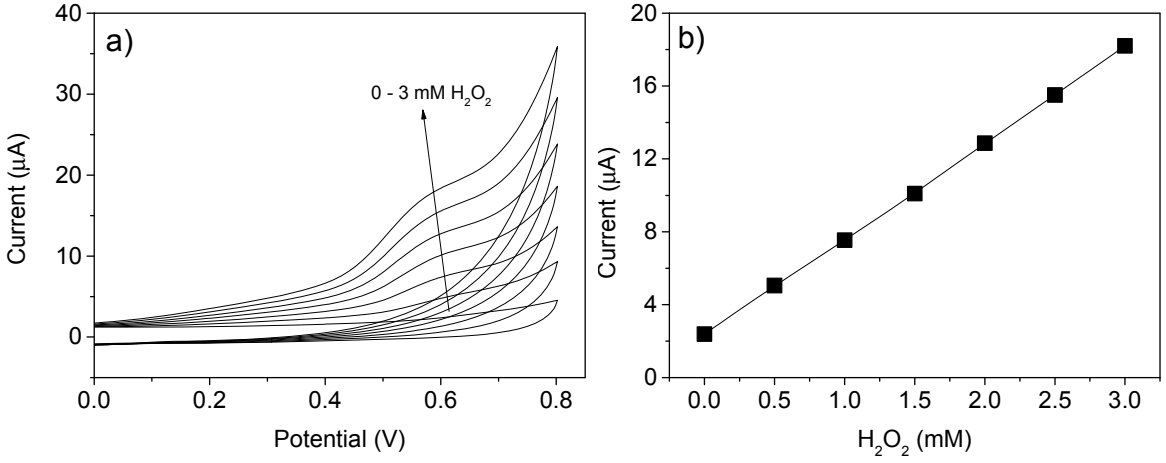


*Figure 4: CVs of the Au/$CeO_2$ nanocomposite in the presence of different concentrations of hydrogen peroxide; b) peak current as function of $H_2O_2$ concentration*

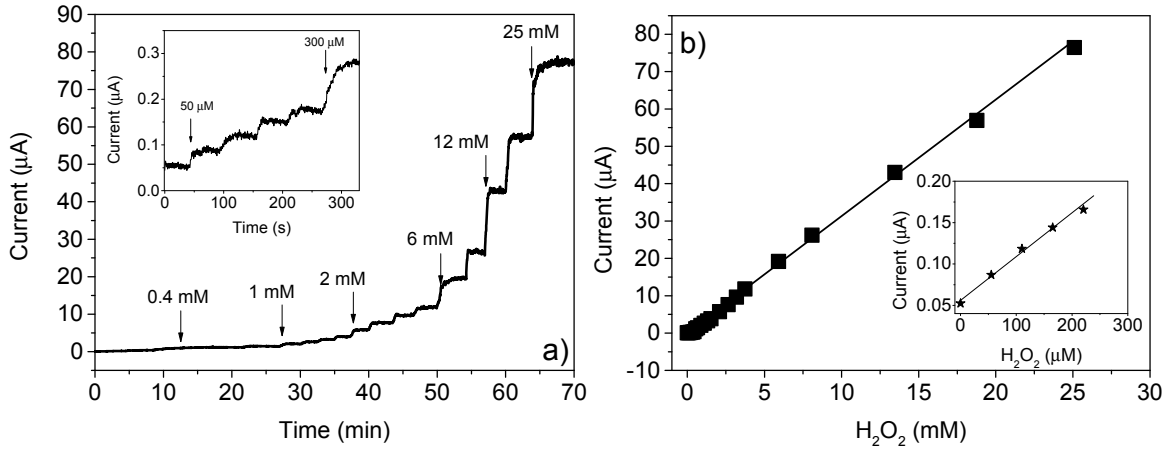


*Figure 5: a) Amperometric response at an applied potential of 0.6 V of the electrode modified with Au/$CeO_2$; b) calibration curve*

Figure 4 shows the effect of $H_2O_2$ concentration on the CV pattern. When increasing the analyte concentration from 0 up to 3 mM, the anodic peak increases in intensity, suggesting the possibility of using electrochemical techniques for quantitative $H_2O_2$ detection.

Chroamperometry was therefore used to test the detection of $H_2O_2$ with the fabricated electrode modified with Au/$CeO_2$ composite. Figure 5a shows the amperometric response, obtained by successive addition of different aliquots of $H_2O_2$ at the constant potential of 0.6 V. The typical current-time curve shows a rapid and sensitive response of the modified electrode to the change in $H_2O_2$ concentration. The corresponding calibration curve (Figure 5b) exhibits an excellent linear response within range from 0 to 30 mM. Moreover, a detection limit of 5 μM (based on S/N = 3) and a sensitivity of 27.1 A $mM^{-1}$ $cm^{-2}$ were measured.

In order to explain the enhanced effect of the Au/$CeO_2$ composite compared to $CeO_2$ and to bare carbon electrode, we can consider: i) the electron-transfer ability of the Au/$CeO_2$ composite and ii) the higher electro-activity for $H_2O_2$ provided by the Au nanoparticles. Furthermore, in general, for noble-metal-loaded/metal oxides, the electrochemical properties largely depend on the preparation method, on the surface physicochemical properties and even on the thermal processes adopted. The $CeO_2$ surface characteristics (such as exposed crystal facets, surface defects, etc.) should also be deeply considered. Meanwhile, the size of the noble metal clusters on the surface is also a crucial factor. Further investigations are planned in order to get a better understanding of the influence of all these variables on the electrocatalytic properties of the Au/$CeO_2$ composite towards $H_2O_2$.

## 4. Conclusions

In this contribution we reported on the fabrication of $H_2O_2$ sensors based on Au nanoparticles dispersed on $CeO_2$ by a deposition-precipitation method. The electrochemical sensor was manufactured by printing the Au/$CeO_2$ composites onto commercial carbon-based planar electrodes and tested by cyclic voltammetry in the presence of $H_2O_2$ to evaluate its electrochemical performances.

The results showed that the fabricated sensor displayed good performance in terms of sensitivity and linear response, for the detection of $H_2O_2$. An anodic peak current was observed on the Au/$CeO_2$ modified electrode as opposed to the unmodified carbon electrode, which was ascribed to the better electron-transfer ability and/or the higher electro-activity provided by the Au/$CeO_2$ hybrid composite sensing layer. The developed enzyme-free Au/$CeO_2$ sensor exhibited a linear response to $H_2O_2$ in the range investigated (0-3 mM) with a sensitivity of about 27.1 μA $mM^{-1}$ $cm^{-2}$, which is suitable for a variety of industrial applications.

### References

Ampelli C., Spadaro D., Neri G., Donato N., Latino M., Passalacqua R., Perathoner S., Centi G., 2012, Development of Hydrogen Leak Sensors for Fuel Cell Transportation, Chem. Eng. Trans., 26, 333-338.Ampelli C., Perathoner S., Centi G., 2014a, Carbon-based catalysts: opening new scenario to develop next-generation nano-engineered catalytic materials, Chin. J. Catal., 35 (6), 783-791.

Ampelli C., Leonardi S.G., Genovese C., Lanzafame P., Passalacqua R., Perathoner S., Centi G., Neri G., 2014b, Novel Electrochemical Sensors for Safety and Control in Fermentation Processes, Chem. Eng. Trans., 36, 319-324.

Ampelli C., Genovese C., Lanzafame P., Perathoner S., Centi G., 2014c, A sustainable production of $H_2$ by water splitting and photo-reforming of organic wastes on Au/$TiO_2$ nanotube arrays, Chem. Eng. Trans., 39, 1627-1632.

Ampelli C., Genovese C., Passalacqua R., Perathoner S., Centi G., 2014d, A gas-phase reactor powered by solar energy and ethanol for $H_2$ production, Appl. Therm. Eng., 70, 1270-1275.

Chen W., Cai S., Ren Q.-Q., Wen W., Zhao Y.-D., 2012, Recent advances in electrochemical sensing for hydrogen peroxide: a review, Analyst, 137, 49-58.

Ensafi A.A., Zandi-Atashbar N., Ghiaci M., Taghizadeh, M., Rezaei B., 2015, Synthesis of new copper nanoparticle-decorated anchored type ligands: Applications as non-enzymatic electrochemical sensors for hydrogen peroxide, Mater. Sci. Eng. C, 47, 290-297.

Ispas C., Njagi J., Cates M., Andreescu S., 2008, Electrochemical Studies of Ceria as Electrode Material for Sensing and Biosensing Applications, J. Electrochem. Soc., 155, F169-F176.

Jones C.W., Eds., 1999, Applications of Hydrogen Peroxide and Derivatives, The Royal Society of Chemistry, Cambridge, UK.

Leonardi S.G., Aloisio D., Donato N., Russo P.A., Ferro M.C., Pinna N., Neri G., 2014, Amperometric Sensing of $H_2O_2$ using Pt-$TiO_2$/Reduced Graphene Oxide Nanocomposites, ChemElectroChem, 1, 617- 624.

Kim G., Lee Y.-E.K., Kopelman R., 2013, Hydrogen peroxide ($H_2O_2$) detection with nanoprobes for biological applications: A mini-review, Method. Mol. Biol., 1028, 101-114.

Palard M., Balencie J., Maguer A., Hochepied J.F., 2010, Effect of hydrothermal ripening on the photoluminescence properties of pure and doped cerium oxide nanoparticles, Mater. Chem. Phys., 120, 79-88.

Signoretto M., Menegazzo F., Contessotto L., Pinna F., Manzoli M., Boccuzzi F., 2013, Appl. Catal. B-Environ., 129, 287- 293.

Tong Y., Li Z., Lu X., Yang L., Sun W., Nie G., Wang Z., Wang C., 2013, Electrochemical determination of dopamine based on electrospun $CeO_2$/Au composite nanofibers, Electrochim. Acta, 95, 12-17.

Ujjain S.K, Das A., Srivastava G., Ahuja P., Roy M., Arya A., Bhargava K., Sethy N., Singh S.K., Sharma R.K., Das M., 2014, Nanoceria based electrochemical sensor for hydrogen peroxide detection, Biointerphases, 9 (3), 031011, DOI: 10.1116/1.4890473.

Yin J., Qi X., Yang, L., Hao G., Li J., Zhong J., 2011, A hydrogen peroxide electrochemical sensor based on silver nanoparticles decorated silicon nanowire arrays, Electrochim. Acta, 56 (11), 3884-3889.

Zhang W., Xie G., Li S., Lu L., Liu B., 2012, Au/$CeO_2$–chitosan composite film for hydrogen peroxide sensing, Appl. Surf. Sci., 258, 8222-8227.

Zhao W., Wang H., Qin X., Wang X., Zhao Z., Miao Z., Chen L., Shan M., Fang Y., Chen Q., 2009, A novel nonenzymatic hydrogen peroxide sensor based on multi-wall carbon nanotube/silver nanoparticle nanohybrids modified gold electrode, Talanta, 80, 1029-1033.